

NASA/CR 91- 206029

NAG9-785

11/30/95

093222

FINAL REPORT

AMMONIA LEAK LOCATOR STUDY

Prepared by

**Franklin T. Dodge
Martin P. Wüest
Danny M. Deffenbaugh**

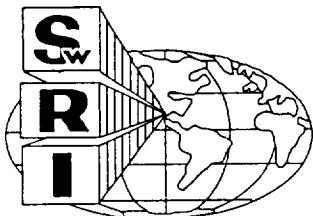
November 1995

SwRI Project 04-7218

Prepared for

**Dr. John Graf
NASA Johnson Space Center
Mail Code EC3
2101 NASA Road 1
Houston, TX 77058-3696**

NASA Grant No. NAG 9-785



SOUTHWEST RESEARCH INSTITUTE

**SAN ANTONIO
DETROIT**

**HOUSTON
WASHINGTON, DC**

SOUTHWEST RESEARCH INSTITUTE
P.O. Drawer 28510
San Antonio, Texas 78228-0510

FINAL REPORT

AMMONIA LEAK LOCATOR STUDY

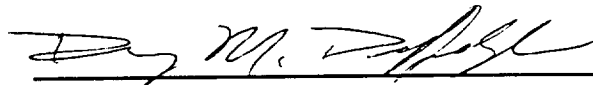
November 1995

SwRI Project 04-7218

Prepared for

Dr. John Graf
NASA Johnson Space Center
Mail Code EC3
2101 NASA Road 1
Houston, TX 77058-3696

Approved:



Danny M. Deffenbaugh, *Director*
Mechanical and Fluids Engineering Division

TABLE OF CONTENTS

Executive Summary.....	1
1.0 Introduction.....	2
2.0 Space Station External Environment	3
2.1 External Environment.....	3
2.1.1 Natural sources.....	3
2.1.2 Offgassing and venting sources.....	4
2.1.3 EVA sources.....	4
2.1.4 Ammonia sources.....	4
3.0 Prediction of Representative Ammonia Leak Characteristics.....	12
3.1 Model of Ammonia Leaking from a Small Hole into Infinite Space.....	12
3.1.1 Physical description of vapor plume generation.....	12
3.1.2 Analytical model.....	12
3.2.3 Predicted vapor plume pressure and density.....	13
3.3 Model of Ammonia Leaking from a Small Hole into a Tray or Channel.....	14
3.3.1 Analytical model.....	15
3.3.2 Choked flow pressure.....	15
3.3.3 Time to obtain steady state.....	15
3.3.4 Predicted plume pressure.....	16
3.4 Summary.....	16
4.0 Ion Gauge Capabilities Survey.....	17
4.1. Hot Ionization Gauges.....	17
4.1.1 Measurement principle.....	17
4.1.2 Conventional triode.....	17
4.1.3 Bayard-Alpert.....	18
4.1.4 Accuracy of hot ion gauges.....	18
4.1.5 Size.....	19
4.1.6 Power requirements.....	19
4.2 Cold Cathode.....	19
4.2.1 Principle of operation.....	19
4.2.2 Advantages and limitations.....	21
4.4 Photoionized Ion Gauge.....	21
4.4.1 Principle of operation.....	21
4.4.2 Size.....	21
4.4.3 Power.....	21
4.5 Semiconductor Ion Gauge.....	21
4.6 Selectivity to Ammonia.....	21
4.7 Advantages and Disadvantages.....	21
5.0 Evaluation of Baseline and Alternative Ammonia Leak Detection Methods.....	23

5.1 Instruments Evaluated..... 23

5.2 Trade Study of Ammonia Leak Instruments 23

5.3 Discussion of Trade Study Scores 23

 5.3.1 Ion gauge..... 23

 5.3.2 Selective ion gauge 25

 5.3.3 Mass spectrometer 25

 5.3.4 Infrared absorption gauge..... 26

 5.3.5 Infrared fluorescence gauge 28

 5.3.6 Disclosing paint gauge 28

6.0 Conclusions and Recommendations..... 29

References 30

LIST OF FIGURES

Figure	Page
1.1 Operating Principle of An Ion Gauge.....	2
3.1 Vaporization of a Liquid Jet and Subsequent Supersonic Expansion of the Vapor Plume into a Vacuum.....	12
3.2 Pressure and Density of an Ammonia Plume Resulting from a Leak into an Infinite Space. $K = 0.2$	14
3.3 Schematic Illustration of Channel/Tray Ammonia Leak Model.....	15
3.4 Pressure Buildup in a 1m X 1m X 30m Channel for Various Leak Rates. $K = 0.2$	16
3.5 Distance from a Channel at Which the Vapor Plume Pitot Total Pressure Drops to a Background Pressure of 10^{-6} Torr	16
4.1 Schematic of a High Pressure Triode Ionization Gauge [adapted from Wüest (1987)]..	17
4.2 Schematic of a Bayard-Alpert Ion Gauge	18
4.3 Schematic Electronics Set-up for a Hot Ion Gauge	19
4.4 Cut-Away Diagram of a Cold Cathode Ion Gauge and Associated Circuit (after Hobson and Redhead, 1958).	19
5.1 Schematic of a Ammonia Leak Location Gauge Based on Infrared Absorption (not to scale)	27
5.2 Schematic of a Laser-Induced Fluorescence Ammonia Leak Location Gauge (not to scale)	28

LIST OF TABLES

Table	Page
2.1 Earth Thermal and Pressure Parameters.....	3
2.2 ISSA Vents (6/15/95)	5
3.1 Summary of Analytical Model for Ammonia Leaking into an Infinite Space	13
3.2 Summary of Plume Pressure and Density Predictions	14
3.3 Pressure (Torrs) Required to Cause Flow Through a Hole to be Choked.....	15
4.1 Typical Values of Hot Ionization Gauges.....	20
4.2 Comparison of Ion Gauges	22
5.1 Instruments Evaluated in Trade Study	23
5.2 Ammonia Leak Locator Trade Study	24

Executive Summary

Leaks of ammonia in the thermal control system of the International Space Station Alpha (ISSA) must be detected and located before the supply of ammonia becomes critically low. Although the *existence* of a leak can be detected by various monitoring systems, determining the *location* of the leak is a difficult technical challenge because the vapor plume from the leak is commingled with the gases and vapors from a variety of vents and offgassing sources that form an atmosphere around ISSA with a background pressure as large as 10^{-6} torr.

Baseline instrument. Initially, NASA selected an ion gauge as the ISSA baseline ammonia leak-location instrument. An ion gauge is a technology-ready device, and it can be packaged into a hand-held instrument for use during extra-vehicular activities to locate leaks. Such a gauge actually detects the pressure (or density) of the gas for which it is calibrated. Therefore, if an ammonia leak is to be located successfully, the pressure of the ammonia vapor plume must be substantially greater than the background pressure of the ISSA environment. Analytical models developed in this study showed, however, that the partial pressure of an ammonia vapor plume, for anticipated leak rates of 0.5 to 1.5 lbs/day, decreased to below the background pressure within a distance of only several feet of the leak. Because of the need, therefore, to be quite close to the leak source to detect it, the success of an ion gauge as an ammonia leak locator is problematical.

Ammonia-specific instruments. Based on this analysis of ion gauges, coupled with the large number of gases and vapors in the ISSA environment and the relatively large background pressure of the environment, it appeared that a successful leak-location gauge requires the measurement or detection of some property that was specific to ammonia, in order to distinguish the ammonia vapor plume from the environment.

Instrument trade study. To evaluate the possibility of developing an ammonia-specific gauge, a survey of the capabilities of a large number of potential instruments or location methods was conducted. The instrument and methods represented a wide range of physical principles and technology readiness. Gauges based on five different techniques were then compared to the baseline ion gauge in terms of selectivity for ammonia, complexity, development cost, size, and other relevant parameters.

- "selective" ion gauge
- mass spectrometer
- infrared absorption gauge
- infrared fluorescence gauge
- disclosing paint

The parameters used in this trade study and the weights (importance relative to other parameters) assigned to them were selected in conjunction with NASA. Scores were awarded to each instrument for each traded parameter by a review panel who had demonstrated expertise in designing, fabricating, and using such instruments.

Trade study conclusions. The trade study indicated that a **mass spectrometer** was clearly the best choice for an ammonia leak location instrument and that leak-location instruments based on a "selective" ion gauge and on disclosing paint were also feasible but represented considerably more development risk.

Although there have been previous attempts to develop a mass spectrometer for similar applications with only limited success, recent developments in miniaturization and other improvements indicate that the development of an ammonia leak-location instrument, somewhat similar to available commercial mass spectrometers, should not now be difficult. Therefore, the recommended instrument for the location of ammonia leaks for ISSA is a miniature mass spectrometer.

1.0 Introduction

The thermal control system of International Space Station Alpha will use liquid ammonia as the heat exchange fluid. It is expected that small leaks (of the order perhaps of one pound of ammonia per day) may develop in the lines transporting the ammonia to the various facilities as well as in the heat exchange equipment. Such leaks must be detected and located before the supply of ammonia becomes critically low. For that reason, NASA-JSC has a program underway to evaluate instruments that can detect and locate ultra-small concentrations of ammonia in a high vacuum environment. To be useful, the instrument must be portable and small enough that an astronaut can easily handle it during extravehicular activity. An additional complication in the design of the instrument is that the environment immediately surrounding ISSA will contain small concentrations of many other gases from venting of onboard experiments as well as from other kinds of leaks. These other vapors include water, cabin air, CO₂, CO, argon, N₂, and ethylene glycol. Altogether, this local environment might have a pressure of the order of 10⁻⁷ to 10⁻⁶ torr.

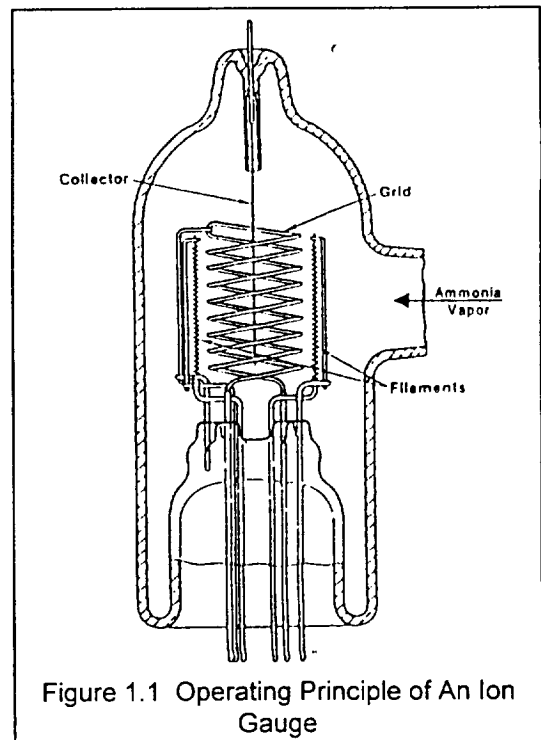
Southwest Research Institute (SwRI) was contracted by NASA-JSC to provide support to NASA-JSC and its prime contractors in evaluating ammonia-location instruments and to make a preliminary trade study of the advantages and limitations of potential instruments. The present effort builds upon an earlier SwRI study to evaluate ammonia leak detection instruments [Jolly and Deffenbaugh, 1989]. The objectives of the present effort include:

1. Estimate the characteristics of representative ammonia leaks.
2. Evaluate the baseline instrument in the light of the estimated ammonia leak characteristics.
3. Propose alternative instrument concepts.
4. Conduct a trade study of the proposed alternative concepts and recommend promising instruments.

The baseline leak-location instrument selected by NASA-JSC was an ion gauge. A typical Bayard-Alpert type of ion gauge is shown schematically in Figure 1.1. The operation of an ion gauge is summarized as follows:

- the filaments are heated so as to emit electrons
- the electrons are accelerated through the voltage difference between the filaments and the grid
- molecules from the gas to be detected, which enter the gauge as shown in the sketch, collide with the electrons and become positively ionized
- the positive ions are attracted to the negatively-charged collector
- the collector current, which is proportional to the density (or pressure) of the detected gas, is monitored to detect the presence of the gas.

An ion gauge, although relatively simple, cannot identify the species of the gas being detected, merely its density or pressure. Thus, it can locate an ammonia leak only if the density or pressure of the ammonia vapor from the leak is sufficiently greater than the background gas density. This physical limitations places a geometric limit on how close the gauge must be to a leak in order to locate it.



2.0 Space Station External Environment

2.1 External Environment

The environment external to the International Space Station Alpha (ISSA) can be attributed to many sources including: natural sources, offgassing of external ISSA hardware, venting events, EVA activities, and leaks of ISSA fluid lines. Ammonia leaking from the Thermal Control System (TCS) will be one contributor to the external environment, but leak detection will require that ammonia leaks be distinguished from other contributors.

2.1.1 Natural sources

Natural sources are those parts of the external atmosphere that are not attributed to ISSA hardware or activities. Table 2.1, taken from the Space Station Program Natural Environment Definition for Design [SSP 30425 Rev B] lists total pressure trends and ranges as a function of altitude. ISSA altitudes range from 225 km to 300 km. The molecular composition of the natural atmosphere in this region of the thermosphere is not specified in SSP 30425; the primary components are N₂, O₂, O, H, and He. Generally, heavier species like N₂ and O₂ persist at lower altitudes, and lighter species are found at higher altitudes. Whenever thermospheric gas is heated, it expands radially outward; thus, the daytime thermospheric density is greater than the nighttime density. Geomagnetic storms also affect density profiles. The natural atmosphere at ISSA altitudes can vary from approximately 1.0⁻⁸ to 1.0⁻⁶ torr. Changes are complex and attributable to changes in altitude, diurnal cycle, and geomagnetic activity.

**Table 2.1 Earth Thermal and Pressure Parameters
Ambient Pressure in Pascal, Torr in parenthesis (Note 1):**

Minimum	Nominal	Maximum	Altitude (km)
1.8E-6 (1.4E-8)	8.8E-6 (6.6E-8)	4.8E-5 (3.6E-7)	300
1.7E-7 (1.3E-9)	1.5E-6 (1.1E-8)	1.5E-5 (1.1E-7)	400
3.6E-8 (2.7E-10)	3.1E-7 (2.3E-9)	5.7E-6 (4.3E-8)	500
1.6E-8 (1.2E-10)	8.3E-8 (6.2E-10)	2.4E-6 (1.8E-8)	600
4.2E-9 (3.2E-11)	7.5E-9 (5.6E-11)	1.3E-7 (9.8E-10)	1000
1.0E-11 (7.5E-14)			Geosynchronous

Notes:

1. Orbit average values of low and high pressure were estimated with the MET Model for a 51.6° inclination orbit, assuming the following input conditions:

Low Pressure Case: (less than 0.2 percentile frequency of occurrence)

F10B = 70, F10 = 70, $a_p = 0$, Ascending node = 150° (orbit intersects solar bulge), Date = July 30, (primary minimum of semiannual variation).

High Pressure Case: (exceeds 99.99 percentile frequency of occurrence)

F10B = 243, F10 = 273, $a_p = 234$, Ascending node = 255° (orbit intersects solar bulge), Date = Oct. 28, (primary maximum of semiannual variation).

Nominal pressure values were taken from U.S. Standard Atmosphere 1976 [Anon., 1976]. Geosynchronous pressure values were taken from [Smith and West, 1982]. To convert from Pascal to Torr multiply by 0.0075.

2.1.2 Offgassing and venting sources

Offgassing of external ISSA hardware is another contributor to the external environment. The Space Station External Contamination Control Requirements Document [SSP 30426] sets the requirement that all materials used in hardware, which will be exposed to space vacuum, shall have a total mass loss of less than 1.0 percent and a volatile condensable material loss of less than 0.1 percent. Offgassing rates will be relatively great initially and decrease as materials age. Offgassed species, and many other external contaminants will have a ram-wake effect. As the space station moves through the earth's rarefied environment, a ram-wake effect is created, with a density buildup on the forward facing surfaces, and a density decrease on the aft facing surface. Buildup on surfaces which have exposure to ram can be as high as 60 times ambient density. It is difficult to quantify the contribution to the external environment caused by offgassing, but offgassing contamination will be greater initially and will decrease with time.

Venting is likely to be the largest contributor to the space station external environment. There are 35 vents on ISSA. Each vent has unique characteristics; some vents will release a single species (such as CO₂ or water). Some vents will vent payload experiments. There are more than 150 organic species that are permitted to be released from these vents. Some vents, like the trace contaminant control system vacuum desorption vent in the Russian module, are entirely unspecified and unregulated. The schedule of venting events is complex and unpredictable. Some vents are released when pressure reaches a set point. Some vents are opened on a regular schedule. Some regularly scheduled vent releases cannot easily be rescheduled because they are directly tied to life support hardware. Amounts of vented material are generally unspecified, but there is some data that can describe the magnitude of venting. All metabolic CO₂ is vented, and a crew of 6 produces 6.0 kg/day of CO₂. Periodic water dumps are scheduled, and each scheduled release vents up to 25 kg of water. Table 2.2 is a listing and description of each ISSA vent. This list was made by the ECLSS AIT (Carlos Soares).

2.1.3 EVA sources

EVA activities contribute to the ISSA external environment. Each time the airlock is opened, approximately 2 kg of gas are released to the outside. The spacesuit uses a water sublimator to control the thermal environment, and approximately 3 kg of water is boiled away during each EVA. The water that is sublimated is in the immediate proximity of the EVA astronaut.

2.1.4 Ammonia sources

Ammonia leaks are the target that must be distinguished from the background. As described previously, a 1.5 lb/day leak is the required leak location capability, and leak location will be done by EVA inspection. Approximately 80% of an ammonia leak will jet away and not be detectable, leaving a residual 0.3 lb/day leak as the target. CO₂ vents located within 1 meter of ammonia lines will release up to 6 kg/day. Water dumps of 25 kg/release will occur. The water sublimator on the EVA space suit will release about 3 kg/EVA, and the release will be in the immediate vicinity of the leak inspection. The natural background is large (on the same order as an ammonia plume 1 meter from the leak) and variable (two orders of magnitude variance). Finding an ammonia leak based on total pressure measurement alone would be extremely difficult because the external environment pressure is large, complex, and variable.

Table 2.2 ISSA Vents (6/15/95)

ISSA/Orbiter Vent Data 6/15/95														
Vent #	Vent Designation	ISSA Location	Vent Name	Vent Coord. X (in)	Vent Coord. Y (in)	Vent Coord. Z (in)	Direction Vector X (in)	Direction Vector Y (in)	Direction Vector Z (in)	Vent Type	Vent Geometr	Operational Flow Rate	Operational Frequency	Can Vent be Scheduled? (Y/N)
		Notes		1	1	2	2	2	3	4	5	6	6	
1	LAB1a LAB1b	US Lab	Vacuum Exhaust System (VES) "T" vent	-72.16	-76.69	227.65	0 0	-0.423 0.423	-0.906 0.906	T	2.5" internal diameter, 1.77" internal diameter branches on T-vent	L.AB1a: 998 g/s (2.2 lbm/s) L.AB1b: 998 g/s (2.2 lbm/s) (Blowdown of 250 liters @ 40 psia to 10E-3 Torr in approx. 15 min)	User defined. Only 1 experiment can use vent at any given time. Unconfirmed venting schedule of up to 900 venting events/year (2.5/day).	
2	LAB2a	US Lab	Condensate water (1/2)	220.30	-53.12	121.49	0	-0.607	-0.794	S	0.055" internal diameter	18 g/s	Vent simultaneous w/LAB2b vent.	Y
3	LAB2b	US Lab	Condensate water (2/2)	220.30	53.12	260.43	0	0.607	0.794	S	0.055" internal diameter	18 g/s	Vent simultaneous w/LAB3 vent.	Y
4	L.AB3	US Lab	Vacuum Resource System (VRS)	-72.16	35.69	269.65	0	0.259	0.966	S	2.5" internal diameter	Max. 1.2 liters/sec @ 10E-3 Torr (2x10E-6 g/s)	Vent is always open Usage is user defined. Several experiments can vent at the same time.	N
5	LAB4	US Lab	Carbon Dioxide	-72.67	74.20	237.94	0	0.913	0.407	S	.43" internal diameter, 37" line equivalent length (over 20" of line)	Peak mass flow rate: 0.26 g/s	Once every 2.4 hrs.	
6	HAB1	US Hab	Carbon Dioxide	?	?	?				S	.43" internal diameter	Peak mass flow rate: 0.26 g/s	Once every 2.4 hrs.	
7	HAB2	US Hab	Hydrogen (scar)	?	?	?								

Table 2.2 ISSA Vents (cont'd)

ISSA/Orbiter Vent Date		6/15/95													
Vent #	Vent Designation	ISSA Location	Vent Name	Venting Duration (Min. & Max.)	Time Between Venting Events (Min. & Max.)	Effluent	Temperature	Pressure	Max & Avg Force	Max. & Avg. Impingement Force	Max. & Avg. Impingement Torque	Torque Impulse for each firing			
			Notes:	6	6	7	8	9	10	11	12	13			
1	LAB1a LAB1b	US Lab	Vacuum Exhaust System (VES) "T" vent			Cabin Air, Nobl Gases, CO ₂ , CO, Trace Gases	300°K limit (80°F)	Requirements at inlet interface between vacuum system and experiment cannot exceed 40 psia peak pressure. Nominal pressure at experiment location: 14.7 psia.							
2	LAB2a	US Lab	Condensate water (1/2)	Min: 12 min. Max: 1 hr. 16 min.	Min: Vent ever 3 days Max: It is possible that we will not vent at all if Russians use water.	humidity condensate	Assume cabin ambient temp. 65-80°F	9-13 psia at exit							
3	LAB2b	US Lab	Condensate water (2/2)	Min: 12 min. Max: 1 hr. 16 min.	Min: Vent ever 3 days Max: It is possible that we will not vent at all if Russians use water.	humidity condensate	Assume cabin ambient temp. 65-80°F	9-13 psia at exit							
4	LAB3	US Lab	Vacuum Resource System (VRS)			Cabin Air, Nobl Gases, CO ₂ , CO, Trace Gases	80°F limit	Max: 10E-3 Torr at exit. Should maintain 10E 3 Torr at experiment. Design flux is 1.2X10E-3 Torr liters/sec.							
5	LAB4	US Lab	Carbon Dioxide	2.15 hrs	0.25 hrs	CO ₂	Stagnation Temp. = 65-80°F; Static Temp. = 0°F	Peak Stagnation Press. = 0.155 psia at exit; Peak Static Press. = 0.085 psia							
6	HAB1	US Lab	Carbon Dioxide	2.15 hrs	0.25 hrs	CO ₂	Stagnation Temp. = 65-80°F; Static Temp. = 0°F	Peak Stagnation Press. = 0.155 psia at exit; Peak Static Press. = 0.085 psia							
7	HAB2	US Hab	Hydrogen (scar)												

Table 2.2 ISSA Vents (cont'd)

ISSA/Orbiter Vent Data														
Vent #	Vent Designation	ISSA Location	Vent Name	Vent Coord. X (in)	Vent Coord. Y (in)	Vent Coord. Z (in)	Direction			Vent Type	Vent Geometr	Operational Flow Rate	Operational Frequency	Can Vent be Scheduled? (Y/N)
							Vector X (in)	Vector Y (in)	Vector Z (in)					
8	JEM1a JEM1b	JEM-PM	Waste Gas A	342.0	-93.9	238.2	-0.788 0.788	0 0	-0.6157 0.6157	T	0 3/4" (Throat)	JEM1a: 185.5 g/s JEM1b: 185.5 g/s	Max. 5 times/day (depends on user)	
9	JEM2a JEM2b	JEM-PM	Waste Gas B	334.3	-98.4	246.0	-0.788 0.788	0 0	-0.6157 0.6157	T	0 3.5" (Throat)	JEM2a: 5.1x10-5 g/s JEM2b: 5.1x10-5 g/s	Max. 5 times/day (depends on user)	
10	JEM3	JEM-PM	PM Airlock Hatch	376.0	-502.4	207.5	0	-1	0	Hatch	770x900 mm (Hatch Opening)	Blowdown	Average 1 time/week (Max. 2 times/day)	
11	JEM4a JEM4b	JEM-PM	PM Airlock Vent	400.9	-504.4	217.7	1 -1	0 0	0 0	T	0 7 mm (Outlet)	JEM4a: 0.9 g/s (max 3.66 g/s) JEM4b: 0.9 g/s (max 3.68 g/s)	Average 1 time/week (Max. 2 time/day)	
12	JEM5a JEM5b	JEM-PM	PM Vacuum Vent	418.7	-408.3	259.9	0.866 -0.866	0 0	-0.5 0.5	T	0 2.5" (Throat)	JEM5a: 2.98x10-8 g/s JEM5b: 2.98x10-8 g/s	Max. 5 times/day (depends on user)	
13	JEM6a JEM6b	JEM-EF	EF Materials Experiment Vent	551.9	-575.5	288.5	0 0	0 0	1 -1	T	0 1/4" (Outlet)	JEM6a: 0.167 g/s JEM6b: 0.167 g/s	1 time/day, 60 min. duration for each vent	
14	ESA1	APM-FO	Experiment Vent	431.4	108.4	143.2	N/A	N/A	N/A	Radial T		Blowdown 40 psia to 10E-3 mbar	Unconfirmed 3 event per week; 2 blowdown per event	
15	ESA2a	APM-FO	Positive Pressure Relief Valve #1	427.2	108.4	136.3						17 g/s @ 1100 hPa	Contingency: Only active when the APM is isolated from ISSA	
16	ESA2b	APM-FO	Positive Pressure Relief Valve #2	421.4	108.4	141.9						17 g/s @ 1100 hPa	Contingency: Only active when the APM is isolated from ISSA	
17	ESA3a	APM-FO	Depressurization Assembly #1	331.5	108.4	136.3				Radial T		150 g/s @ 1013 mbar	Contingency: Only operated after fire event or atmosphere contamination	
18	ESA3b	APM-FO	Depressurization Assembly #2	326.1	108.4	141.7				Radial T		150 g/s @ 1013 mbar	Contingency: Only operated after fire event or atmosphere contamination	
19	ESA3c	APM-FO	Depressurization Assembly #3	331.6	108.4	147.2				Radial T		150 g/s @ 1013 mbar	Contingency: Only operated after fire event or atmosphere contamination	

Table 2.2 ISSA Vents (cont'd)

ISSA/Orbiter Vent Date		6/15/95		Vent #	ISSA Location	Vent Name	Venting Duration (Min. & Max.)	Time Between Venting Events (Min. & Max.)	Effluent	Temperature	Pressure	Max & Avg Force	Max. & Avg. Impingement Force	Max. & Avg. Impingement Torque	Torque Impulse for each firing
8	JEM1a JEM1b	JEM-PM	Waste Gas A	60 min.	Max. 5 times/day	Cabin Air, Noble Gases, CO ₂ , CO, Trace Gases	20°C	40 psi to 10 torr							
9	JEM2a JEM2b	JEM-PM	Waste Gas B	60 min.	Max. 5 times/day	Cabin Air, Noble Gases, CO ₂ , CO, Trace Gases	20°C	10 torr to 10E-3 torr							
10	JEM3	JEM-PM	PM Airlock Hatch		Average 1 time/week (Max 2 times/day)	Cabin Air	20°C	10 torr (Max. design pressure for hatch mechanism)							
11	JEM4a JEM4b	JEM-PM	PM Airlock Vent	Nominal: 175 sec Max: 174 sec.	Average 1 time/week (Max 2 times/day)	Cabin Air	20°C	152 torr							
12	JEM5a JEM5b	JEM-PM	PM Vacuum Vent	60 min.	Max. 5 times/day	Cabin Air, Noble Gases, CO ₂ , CO, Trace Gases	20°C	under 1x10 ⁻³ torr							
13	JEM6a JEM6b	JEM-EF	EF Materials Experiment Vent	60 min.	1 time/day	Argon	Less than 100°C	0.1 to 1 torr							
14	ESA1	APM-FO	Experiment Vent			Primary: Air, N ₂ ; Secondary: CO ₂ , CO, Noble Gases, Trace Gases		Blowdown 40 psia to 10E-3 mba							
15	ESA2a	APM-FO	Positive Pressure Relief Valve #1			Air						Max: 0.071N in any direction		Max: 0.071N	
16	ESA2b	APM-FO	Positive Pressure Relief Valve #2			Air						Max: 0.071N in any direction		Max: 0.071N	
17	ESA3a	APM-FO	Depressurization Assembly #1			Air, Fire Products, CO ₂ , Toxic/Contaminated Air						Max: 0.058N in any direction		Max: 0.058N	
18	ESA3b	APM-FO	Depressurization Assembly #2			Air, Fire Products, CO ₂ , Toxic/Contaminated Air						Max: 0.058N in any direction		Max: 0.058N	
19	ESA3c	APM-FO	Depressurization Assembly #3			Air, Fire Products, CO ₂ , Toxic/Contaminated Air						Max: 0.058N in any direction		Max: 0.058N	

Table 2.2 ISSA Vents (cont'd)

ISSA/Orbiter Vent Data														
Vent #	Vent Designation	ISSA Location	Vent Name	Vent Coord. X (in)	Vent Coord. Y (in)	Vent Coord. Z (in)	Direction Vector X (in)	Direction Vector Y (in)	Direction Vector Z (in)	Vent Type	Vent Geometry	Operational Flow Rate	Operational Frequency	Can Vent be Scheduled? (Y/N)
20	ESA3d	APM-FO	Depressurization Assembly #4	237.0	108.4	141.7				Radial T		150 g/s @ 1013 mbar	Contingency: Only operated after fire event or atmosphere contamination	
21	ESA4	APM-AF	Experiment Vacuum Resources	378.9	340.1	190.9	N/A	N/A	N/A	Radial T		Continuous Low Pressure (10E-3 mbar)	Unconfirmed 3 event per week; 2 blow-downs per event	
22	RSA1	Service Mobile	TCS							S	Diameter of pipe outlet = .23 in (5 mm)		Once every 6 months	
23	RSA2a		Airlock Chamber/EVA #1							T	Diameter of throat section = .91 in (23 mm)			
24	RSA2b		Airlock Chamber/EVA #2							T	Diameter of throat section = .91 in (23 mm)			
25	RSA2c		Airlock Chamber/EVA #3							T	Diameter of throat section = .91 in (23 mm)			
26	RSA2d		Airlock Chamber/EVA #4							T	Diameter of throat section = .91 in (23 mm)			
27	RSA3a		Airlock Chamber #1								Diameter of throat section = .19 in (5 mm)			
28	RSA3b		Airlock Chamber #2								Diameter of throat section = .19 in (5 mm)			
29	RSA3c		Airlock Chamber #3								Diameter of throat section = .19 in (5 mm)			
30	RSA3d		Airlock Chamber #4								Diameter of throat section = .19 in (5 mm)			
31	RSA4	Service Module	"Vozdukh"	-1,395.8	0.0	217.9				Moment-less nozzle with 4 side holes	Diameter of outlet = 1.96 in (50 mm); throat section area (total) = 20 sq cm	5x10E-3 g/s (Max: 125 l/h)	Continuous	
32	RSA5	Service Module	MPU							Moment-less nozzle with 4 side holes	Diameter of outlet = 1.96 in (50 mm); throat section area (total) = 20 sq cm	0.045 g/s (Max: 125 l/h)	Once every 10 days	

Table 2.2 ISSA Vents (cont'd)

Vent #	Vent Designation	ISSA Location	Vent Name	Venting Duration (Min. & Max.)	Time Between Venting Events (Min. & Max.)	Effluent	Temperature	Pressure	Max & Avg Force	Max. & Avg. Impingement Force	Max. & Avg. Impingement Torque	Torque Impulse for each firing
20	ESA3d	APM-FO	Depressurization Assembly #4			Air, Fire Products, CO ₂ , Toxic/Contaminated Air			Max: 0.058N in any direction		Max: 0.058N	
21	ESA4	APM-AF	Experiment Vacuum Resource			Primary: Air, N ₂ Secondary: CO ₂ , CO, Noble Gases, Trace Gases		Continuous Low Pressure (10E-3 mbar)				
22	RSA1	Service Module	TCS			Ethylene Glycol	-25°C	Pressure of working medium - up to 25 kg/sq cm				
23	RSA2a		Airlock Chamber/EVA #1			Air with Max. 30% O ₂	18-28°C	Initial pressure - 770 mmHg; final pressure - 10 mmHg				
24	RSA2b		Airlock Chamber/EVA #2			Air with Max. 30% O ₂	18-28°C	Initial pressure - 770 mmHg; final pressure - 10 mmHg				
25	RSA2c		Airlock Chamber/EVA #3			Air with Max. 30% O ₂	18-28°C	Initial pressure - 770 mmHg; final pressure - 10 mmHg				
26	RSA2d		Airlock Chamber/EVA #4			Air with Max. 30% O ₂	18-28°C	Initial pressure - 770 mmHg; final pressure - 10 mmHg				
27	RSA3a		Airlock Chamber #1			Air with Max. 30% O ₂	18-28°C	Initial pressure - 770 mmHg; final pressure - 10 mmHg				
28	RSA3b		Airlock Chamber #2			Air with Max. 30% O ₂	18-28°C	Initial pressure - 770 mmHg; final pressure - 10 mmHg				
29	RSA3c		Airlock Chamber #3			Air with Max. 30% O ₂	18-28°C	Initial pressure - 770 mmHg; final pressure - 10 mmHg				
30	RSA3d		Airlock Chamber #4			Air with Max. 30% O ₂	18-28°C	Initial pressure - 770 mmHg; final pressure - 10 mmHg				
31	RSA4	Service Module	"Vozdukh"			80-97% CO ₂ , remainder air & Max: 250 gm H ₂ O per day	10-40°C	Pressure from 60 to 0.3 mmHg				
32	RSA5	Service Module	MPU			Max. 300 gm air; Max: 200 gm of H ₂ O	18-28°C	Pressure from 760 to 00 mmHg				

Table 2.2 ISSA Vents (cont'd)

ISSA/Orbiter Vent Data 6/15/95														
Vent #	Vent Designation	ISSA Location	Vent Name	Vent Coord. X (in)	Vent Coord. Y (in)	Vent Coord. Z (in)	Direction Vector X (in)	Direction Vector Y (in)	Direction Vector Z (in)	Vent Type	Vent Geometry	Operational Flow Rate	Operational Frequency	Can Vent be Scheduled? (Y/N)
33	RSA6	Service Module	"Elektron"	-1,395.8	0.0	107.9				T	Side holes have total area of 12.56 sq cm	8x10E-3 g/s (0-320 l/h, depending on whether the station has a power supply)	once every 10 days	
34	RSA7a	Life Support Module	"Vozdukh"	-1,179.7	-240.4	530.9				Moment-less nozzle with 4 side holes	Diameter of outlet = 1.96 in (50 mm); throat section area (total) = 20 sq cm	7x10E-3 g/s (Max: 160 l/h)	Continuous	
35	RSA8	Life Support Module	"Elektron"	-1,179.7	-240.4	436.9				T	Side holes have total area of 12.58 sq cm	8x10E-3 g/s (0-320 l/h, depending on whether the station has a power supply)	once every 10 days	

3.0 Prediction of Representative Ammonia Leak Characteristics

An analytical predictive model is needed to establish whether it is feasible to locate an ammonia leak by an ion gauge or other instrument that measures only the pressure or density of the vapor plume generated by the leaking liquid ammonia. Two general kinds of ammonia leaks are of interest:

- liquid escaping from a small diameter hole (0.005 in diameter) into an infinite vacuum space having a background pressure of 10^{-6} to 10^{-7} torr; the leak rate is 0.5 to 1.5 lb/day for up to 25 days;
- liquid escaping through a small diameter hole into a representative tray (1 meter by 1 meter channel of various lengths); the ammonia eventually escapes through seams or holes into an infinite space having a background pressure of 10^{-6} to 10^{-7} torr; the leak rate is 0.5 to 1.5 lb/day for up to 25 days.

The background vacuum pressure results from the discharge and venting of liquids and gases from ISSA.

3.1 Model of Ammonia Leaking from a Small Hole into Infinite Space

3.1.1 Physical description of vapor plume generation

Several previous experiments have investigated the characteristics of a water jet flowing through a small orifice into a vacuum [Fuchs and Legge, 1979; Mann and Stoll, 1964; Mikatarian and Anderson, 1965; Steddum, et al, 1970]. The results of these experiments are the basis of the present analytical model of a liquid ammonia leak. The experimental findings are summarized as follows:

- A fraction of the liquid jet flow flashes to vapor (evaporates)
 - the energy removed from the flow (primarily the latent heat) to vaporize the liquid cools the rest of the jet to the point that it freezes a short distance downstream.
- The characteristics of the expanding vapor plume are a strong function of the shape of the orifice
 - when the orifice is “sharp and clean” and there is little gas dissolved in the liquid, the maximum possible fraction of the liquid flow flashes to vapor
 - otherwise, the jet forms a spray and “bursts” and freezes relatively close to the orifice.
- Pressure measurements taken in the plume of flashing vapor [Fuchs and Legge, 1979] show that
 - the vapor expands supersonically in a radial direction
 - the measurements are well predicted by computations based on a continuum gas flow regime
 - exact kinetic theory analysis [Knight, 1976] shows that the continuum flow assumption is reasonable.

A conceptual physical model derived from these experiments is illustrated schematically in Figure 3.1. It is worth noting that, because of the supersonic flow of the expanding vapor, there is a surface at which the flow passes through the sonic velocity [Knight, 1976]; this sonic surface supplies the needed reference quantities for analyzing the pressure and particle density of the expanding vapor [Shapiro, 1953].

3.1.2 Analytical model

To develop an analytical model from the physical model, several assumptions are needed; they are listed below with their justifications:

- The area of the sonic surface is equal to the surface of the liquid fraction of the jet
 - previous computations [Fuchs and Legge, 1979] show that the sonic surface radius is approximately the same as the orifice radius.

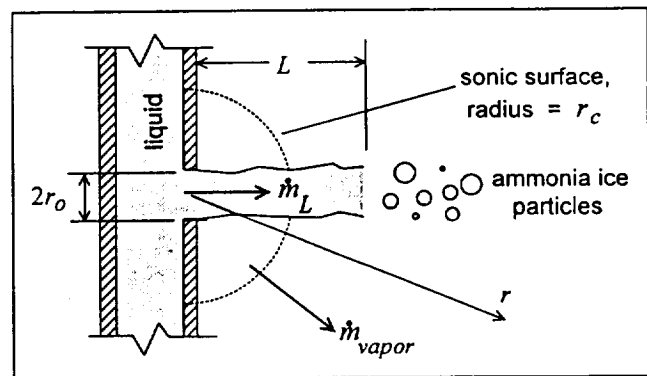


Figure 3.1 Vaporization of a Liquid Jet and Subsequent Supersonic Expansion of the Vapor Plume into a Vacuum

- The length to diameter ratio L/d of the liquid fraction of the jet is approximately 100
 - this ratio agrees roughly with the experiments for jets that did not form a spray near the orifice
 - other ratios can be investigated parametrically (but changing L/d changes only the area of the sonic surface, and the plume characteristics are practically independent of this area).
- For locations distant from the ammonia source ($r/r_o \gg 1$), the plume expansion appears to emanate from a point source
 - this is a reasonable geometric approximation.
- The pressure and density at a point in the plume are computed as if the flow were steady
 - the leak persists for durations long compared to the transient time required for the supersonic plume to reach points that are hundreds of feet away from the leak source, hence, except for a short initial time period, conditions at any specific location do not change with time.
- The vapor plume expands into a perfect vacuum
 - over much of the plume volume, the pressure is orders of magnitude larger than the background pressure, so the partial pressure of the background has a negligible effect on the plume
 - at locations distant from the leak source where the plume pressure is comparable to the background pressure, it is conservative to neglect the background pressure (i.e., the model overpredicts the ability to locate the plume by pressure measurements).
- Processes that remove ammonia molecules from the vapor are neglected
 - these processes are small effects (e.g., interaction of ammonia ions with the earth's magnetic field), so it is conservative to neglect them.

Table 3.1 summarizes the analytical model developed from the conceptual physical model.

3.2.3 Predicted vapor plume pressure and density

The equations shown in Table 3.1 were solved for a range of parameters describing a leak of liquid ammonia at 60°F into an infinite space. Since thermodynamic data for ammonia ice could not be found, the thermodynamic parameter K in the vapor generation equation (see Table 3.1) could not be computed

Table 3.1 Summary of Analytical Model for Ammonia Leaking into an Infinite Space

Equation	Comment
$\frac{\dot{m}_{\text{vapor}}}{\dot{m}_L} = \frac{h_L - h_{\text{ice}}}{h_{\text{vapor}} - h_{\text{ice}}} = K$	Vapor generation rate is given in terms of leak rate and ammonia liquid h_L , vapor h_{vapor} and ice h_{ice} enthalpies (mass and energy conservation)
$r_c = r_o \sqrt{L/r_o} \quad L/r_o = 100$ $P_c = \frac{K \dot{m}_L}{2\pi r_c^2} \left[\frac{2RT_o}{\gamma(\gamma+1)} \right]^{1/2}$	These relations give the effective radius r_c of sonic surface and vapor pressure P_c at the sonic surface. R = ammonia gas constant; T_o = ammonia liquid temperature; γ = ratio of ammonia specific heats
$\frac{1}{M} \left[\frac{2 + (\gamma - 1)M^2}{\gamma + 1} \right]^{\frac{\gamma+1}{2(\gamma+1)}} = \left(\frac{r}{r_c} \right)^2$ $\frac{P}{P_c} = \left[\left(\frac{\gamma+1}{2} \right) \frac{(\gamma+1)M^2}{2 + (\gamma-1)M^2} \right]^{\frac{\gamma}{\gamma-1}} \left[\frac{2\gamma M^2 - (\gamma-1)}{\gamma+1} \right]^{-\frac{\gamma}{\gamma-1}}$	Ideal gas supersonic flow relations that express pressure P and Mach number M in terms of the spherical expansion of the plume. Pressure is the "pitot" total pressure behind a normal shock formed at the inlet to an ion gauge located a distance r from the leak source.
$\rho = \frac{A_g}{17} \left(\frac{P}{RT_o} \right)$	This is the particle density of vapor (molecules/vol). A_g = Avogadro's number; 17 = molecular weight of ammonia vapor.

exactly. But for water at 60°F, $K = 0.14$, so a conservative value of 0.2 was assumed for ammonia. The pressure and density are directly proportional to K , so the results presented below can be easily scaled to other values.

From the analytical model summarized in Table 3.1, the predicted variation of plume pressure and density is shown in Figure 3.2, as a function of distance from the leak source, for three different leak rates of liquid ammonia. For distances $r > 10r_0$, the predictions are not sensitive to the leak orifice size, so the plots also apply to orifice diameters somewhat larger or smaller than the 0.005 inch diameter used in the computations. Since the density and pressure are proportional to the leak rate, results for other values of leak rate can be scaled off the plots.

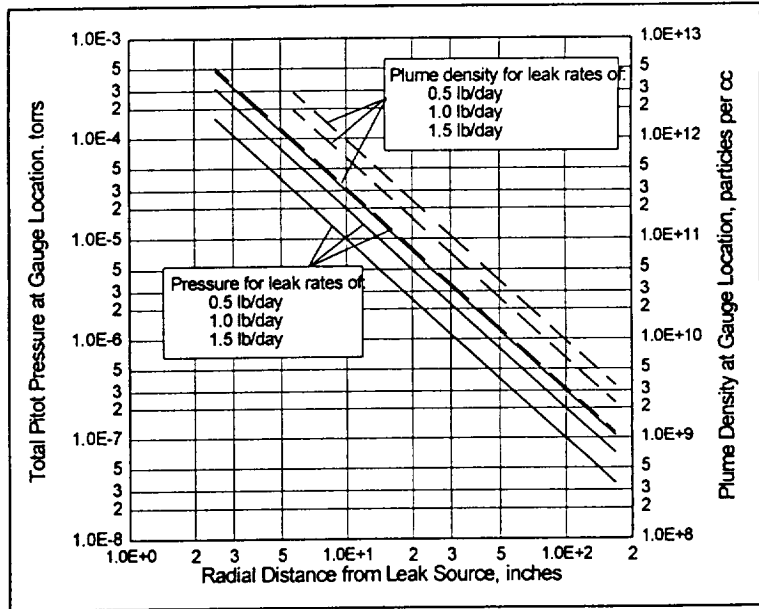


Figure 3.2 Pressure and Density of an Ammonia Plume Resulting from a Leak into an Infinite Space. $K = 0.2$

The plots demonstrate that the “pitot total pressure” of the plume decreases to the background pressure of 10^{-6} or 10^{-7} torr within ten or so feet of the leak source. Hence, it is concluded that the ammonia plume cannot be distinguished from the background on the basis of pressure or density alone unless the measurements are made within several feet of the source.

Table 3.2 summarizes the important results of Figure 3.2 for cases when the background pressure is 10^{-6} torr and 10^{-7} torr.

Table 3.2 Summary of Plume Pressure and Density Predictions

Leak Rate lb/day	Pressure = 10^{-6} torr		Pressure = 10^{-7} torr	
	Distance from leak	Plume density	Distance from leak	Plume density
0.5	32 in	8.4×10^{13} particle/in ³	100 in	8.4×10^{12} particle/in ³
1.0	44 in	8.4×10^{13} particle/in ³	140 in	8.4×10^{12} particle/in ³
1.5	56 in	8.4×10^{13} particle/in ³	175 in	8.4×10^{12} particle/in ³

3.3 Model of Ammonia Leaking from a Small Hole into a Tray or Channel

A likely ammonia leak scenario is (i) an ammonia line develops a hole, (ii) liquid ammonia leaks into the tray or channel holding the lines and flashes into vapor, (iii) the vapor gradually fills up the tray or channel, and (iv) the vapor escapes through a seam or hole in the tray or channel walls into the background vacuum environment of ISSA. The physical processes occurring during this kind of leak are summarized as follows.

- Since the pressure in the tray or channel is typically the same as the background environment, the ammonia liquid flashes into vapor just as if the leak occurred into an infinite vacuum space.
- The flashing vapor expands supersonically until it is confined by the walls of the tray or channel
 - the interaction of the vapor plume and the tray or channel is thereafter a complicated pattern of reflected and transmitted shock waves

- the net effect is that the vapor begins to accumulate and gradually pressurizes the tray or channel volume.
- If the tray walls have at least one leaking seam or micrometeroid puncture, the ammonia vapor begins to escape out of the tray or channel into the effectively infinite background vacuum space.
- The escaping flow rate of vapor gradually increases until it is equal to the rate at which vapor flashes from the liquid jet in the tray or channel
 - the pressure in the tray or channel is then equal to the pressure required to “choke” the vapor venting out the tray or channel (i.e., the velocity of the venting vapor at the leaking seam or puncture is the sonic velocity).

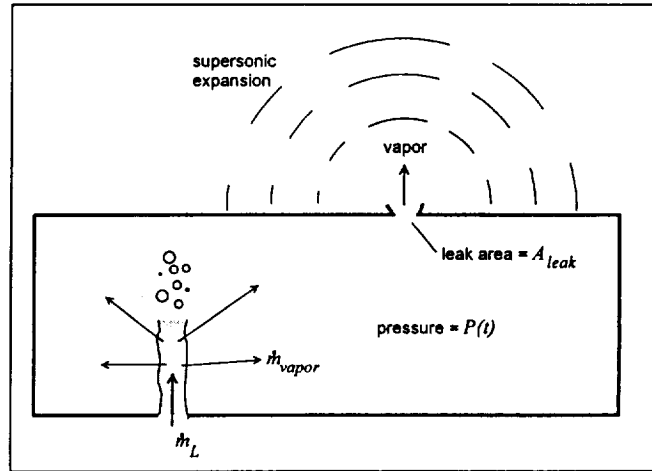


Figure 3.3 Schematic Illustration of Channel/Tray Ammonia Leak Model

- The vapor expands supersonically into an infinite vacuum space (just as if the leaking seam or puncture in the wall was the source of the leak).

Figure 3.3 illustrates this conceptual physical model schematically.

3.3.1 Analytical model

Because of the similarity of these processes to those occurring when ammonia vents directly to an infinite vacuum space, the model summarized previously in Table 3.1 can be used, with some modifications, to predict the plume characteristics for a leak into a tray or channel. It is only necessary to relate the pressure of the accumulated vapor in the channel volume to the area of the leak in the wall (which communicates with the exterior volume) such that the pressure buildup causes the vapor flow out of the tray or channel to be choked.

3.3.2 Choked flow pressure

The sonic flow relations given previously in Table 3.1 can be used to predict the channel volume pressure that is required to cause vapor flowing out through a leak to be choked. Table 3.3 summarizes this required pressure buildup, as a function of the seam or puncture area and total flow rate of vapor flashing in the channel or tray. It should be noted that the total leak areas listed in Table 3.3 can be composed of one or more individual leaks.

3.3.3 Time to obtain steady state

For a constant leak rate into the channel, the channel pressure buildup can be derived from the ideal gas law as a function of time t :

$$P(t) = \left(\frac{K \dot{m}_L R T_o}{V_{tray}} \right) t$$

where V_{tray} is the total interior volume of the tray or channel that can be accessed by the flashing vapor. This relationship neglects the small outflow of vapor through leaks in the wall during the time the pressure builds up to the choked flow condition.

Table 3.3 Pressure (Torrs) Required to Cause Flow Through a Hole to be Choked

Channel Leak Area, in ²	Leak Rate, lb/day		
	0.5	1.0	1.5
0.001	9×10^{-1}	1.9×10^0	2.8×10^0
0.01	9×10^{-2}	1.9×10^{-1}	2.8×10^{-1}
0.1	9×10^{-3}	1.9×10^{-2}	2.8×10^{-2}
1.0	9×10^{-4}	1.9×10^{-3}	2.8×10^{-3}

Figure 3.4 shows a plot of the predicted pressure buildup, for a channel with a total accessible volume of 30 m^3 , as a function of liquid leak rate. From these plots and the data given in Table 3.3, the time required for the pressure to buildup to the point that the vapor flowing out the leak is choked can be obtained. The required time is always on the order of a day or less. Since this is substantially less than the total duration of the leak, the assumption of zero outflow from the channel during the pressure buildup period has a negligible effect on the vapor plume characteristics.

3.3.4 Predicted plume pressure

Since the vapor plume has a sonic surface (at the hole in the channel or tray wall), the supersonic expansion of the plume outside the channel can be computed from the model summarized in Table 3.1. Using this model, Figure 3.5 shows, for example, the distance from the wall at which the pitot total pressure falls to a background pressure of 10^{-6} torr, as a function of vapor leak area and liquid leak rate. These distances are slightly less than if the liquid vented immediately to the infinite space environment. In addition, the supersonic expansion of the vapor plume outside the channel or tray is practically independent of the area of the leak in the channel or tray wall, except in the near vicinity of the leak.

It should be noted that the predictions given in Figure 3.5 assume a single leak in the wall through which all the vapor flows. If there is more than one hole in the walls, the flow through each leak will be proportional to the leak area, and the appropriate distance to the location where the pressure in the plume from a specific leak is equal to 10^{-6} torr should be scaled or interpolated from Figure 3.5.

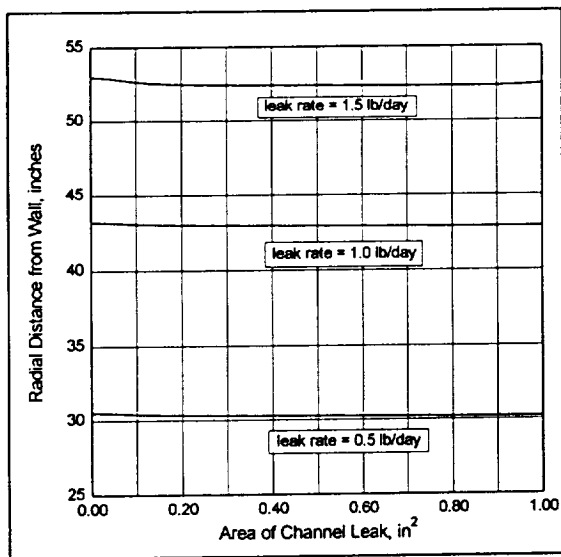


Figure 3.5 Distance from a Channel at Which the Vapor Plume Pitot Total Pressure Drops to a Background Pressure of 10^{-6} Torr

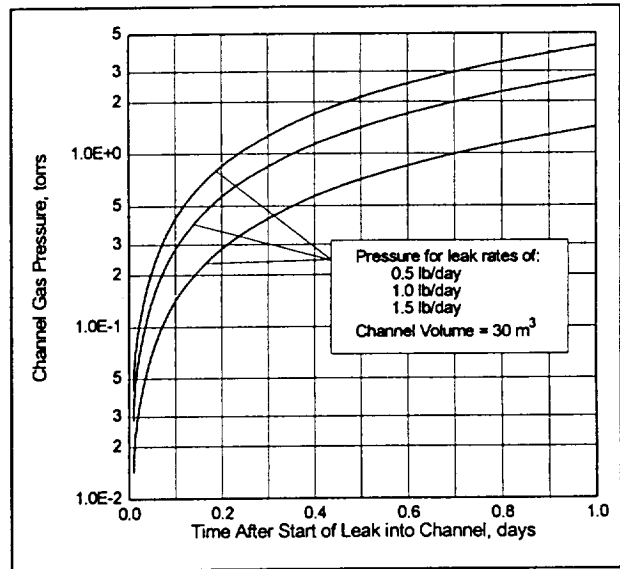


Figure 3.4 Pressure Buildup in a $1 \text{ m} \times 1 \text{ m} \times 30 \text{ m}$ Channel for Various Leak Rates. $K=0.2$

3.4 Summary

The predictions summarized in this Section demonstrate that the pressure in a plume of ammonia vapor falls to the background vacuum pressure within about three to five feet of the leak source when the background pressure is 10^{-6} torr, and within about eight to fifteen feet when the background pressure is 10^{-7} torr. These predictions are valid both for (i) leaks in which liquid ammonia escapes directly into an infinite vacuum space, and (ii) leaks in which liquid ammonia first escapes into a tray or channel and then ammonia vapor vents through a puncture or seam in the walls of the tray or channel into an infinite space. In the second case, the distances at which the plume pressure falls to the background pressure pertain to the distance from the hole or puncture in the tray or channel wall.

The analytical models used to make these predictions are based on (i) physically-justifiable but

experiments on the vapor plumes generated by small-diameter jets of liquid water escaping into a vacuum. For these reasons, the analyses are not theoretically "exact." However, the analytical models are considered to give reasonable predictions (say, within about $\pm 25\%$) of the true plume characteristics.

From the analyses summarized above, the following important conclusion can be drawn:

- any instrument, such as an ion gauge, that relies on pressure or density measurements alone, can locate ammonia leaks of 0.5 to 1.5 lb/day **only** if the instrument is within three to five feet of the leak source (for a background pressure of 10^{-6} torr) or within eight to fifteen feet of the leak source (for a background pressure of 10^{-7} torr).

4.0 Ion Gauge Capabilities Survey

An ion gauge is a pressure device, which is routinely used to measure the total pressure in vacuum chambers. Several different types of gauges have been built. They are distinguished through the method used to ionize the charged particles that provide the basis for a pressure determination. Such methods include the fluorescence gauge, discharge tube, hot and cold ionization gauges, and others.

The most popular ion gauges today are the hot and cold ionization gauges on which we will mainly concentrate. There are two different types: the cold cathode and the hot cathode ion gauge. The hot cathode ion gauges can further be classified by conventional triode and Bayard-Alpert ion gauge approaches. The appropriate type selected depends on several factors, such as the pressure range.

4.1. Hot Ionization Gauges

4.1.1 Measurement principle

The measurement principle of a hot cathode ionization gauge relies on gas ionization. Emitted electrons from the hot cathode collide with gas molecules in the active region of the gauge, ionize some of them and produce a measured ion current. The ion I^+ current is given by

$$I^+ = KI^- \rho \quad (1)$$

where K is a calibration or sensitivity factor, I^- is the ionizing electron current, and ρ is the molar gas density. Therefore, in principle a hot ionization gauge measures a density. If the temperature of the gas is known, the pressure P can be determined from the density, and Eq. (1) becomes

$$I^+ = KI^- \frac{P}{RT} = CI^- P \quad (2)$$

where T is the temperature and R the gas constant. It should be pointed out that the distinction between Eqs. 1 and 2 is important when the gauge is calibrated or specified for a gas at one temperature and used with a gas of another temperature.

4.1.2 Conventional triode

A schematic of a triode design is shown in Figure 4.1.

The use of a thoriated iridium filament as a cathode in a conventional triode usually covers the pressure range from 10^{-6} to 1 mbar. However, Weinmann (1966) designed a gauge which can be operated at pressures between 0.003 and 5.33 mbar.

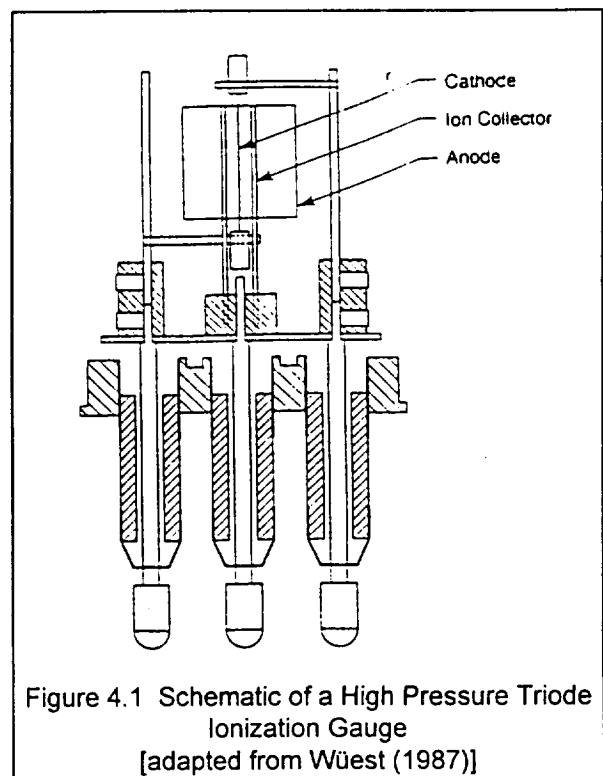


Figure 4.1 Schematic of a High Pressure Triode Ionization Gauge
[adapted from Wüest (1987)]

The conventional triode is limited in its measurement of low pressures by soft x-rays generated from electron impact at the grid. When the x-rays strike the large collector, photoelectrons are emitted. The photoelectrons cannot be distinguished from the ions, giving rise to an apparent pressure-independent ion current.

The upper pressure limit is derived through the reaction of oxygen at the hot tungsten cathode ($T > 2000\text{ K}$), which dissociates molecular oxygen forming atomic oxygen. Atomic oxygen reacts with the carbon impurities of the cathode to yield CO and CO₂. CO₂ is continuously generated as a result of carbon at the surface of the cathode diffusing from the bulk. Oxygen atoms interact with the tungsten cathode and produce WO₂ and WO₃ as surface species which, depending on temperature, interact with each other to yield W₂O₆ and W₃O₉. The tungsten oxide is thereby deposited in the walls of the gauge head.

Atomic hydrogen reduces the tungsten oxide film, setting free water vapor. However, H₂O dissociates at the hot tungsten cathode to form oxygen and atomic hydrogen initiating a vapor cycle. This eventually results in a subsequent reduction of the tungsten cathode thickness.

In a laboratory environment, the higher the total pressure, the higher is the partial pressure of oxygen. This will lead to a quicker decay of the cathode. The service life of tungsten cathodes is 10-20 h at $10^{-2} - 10^{-3}$ mbar and about 1000 h at about 10^{-6} mbar.

Thoria-coated iridium filaments do not burn out when being exposed for a short time during operation to a sudden air in-rush.

4.1.3 Bayard-Alpert

In a Bayard-Alpert (BA) gauge, the positive accelerator grid (anode) is concentrically arranged as a spiral coil around the very thin central ion collector. The inverted triode structure of a BA greatly reduces the x-ray cross-section of the collector while retaining a high ion collection efficiency.

A BA gauge operates typically from 10^{-3} mbar down to approximately 10^{-12} mbar and can be extended through the use of a modulator down to approximately 10^{-13} mbar. The lower limit is again given by the x-ray limit. A schematic of a BA ion gauge is shown in Figure 4.2.

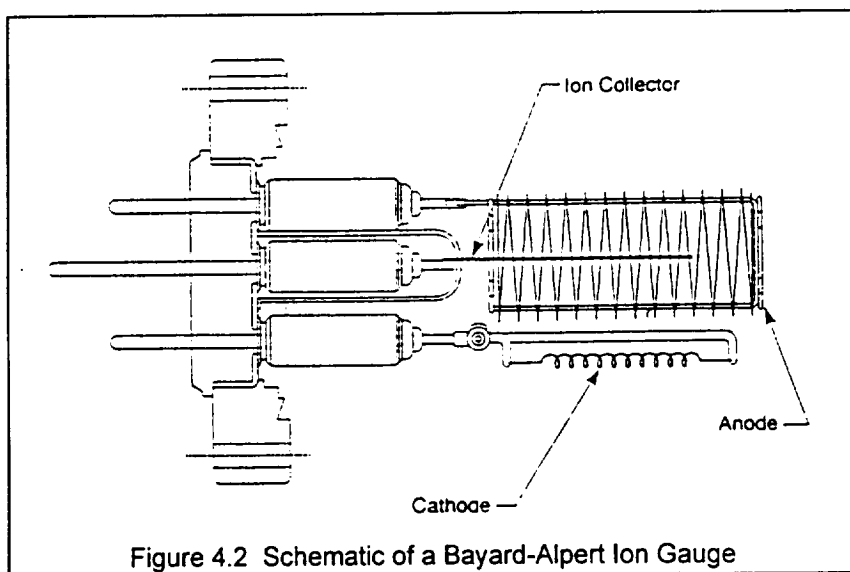


Figure 4.2 Schematic of a Bayard-Alpert Ion Gauge

At high pressures, the collection efficiency is reduced because of the space charge in the vicinity of the ion collector and the sensitivity is no longer linear with pressure.

4.1.4 Accuracy of hot ion gauges

The calibration factor K or C depends among other things on gas species, electron energies, electrostatic field distributions within the gauge structure, temperature, charge densities, and the surface condition of the electrodes. These factors can change with time and conditions of use.

Numerous studies [Tilford, 1983; Redhead, 1969; McCulloh and Tilford, 1981; Poulter and Sutton, 1981] have shown Bayard-Alpert (BA) type gauges to have an associated measurement uncertainty of 30 to 40%. These inaccuracies are inherent in the design of the BA gauge and cannot be consistently compensated for by any controller.

Absolute accuracy of measurement is mainly determined by the condition of the gauge head. If the gauge head is highly contaminated, it can be as much as a factor of 2.

4.1.5 Size

Commercially available hot ion gauges for installation at a vacuum chamber have a length of $\approx 56 - 83$ mm above the mounting flange, but smaller ion gauges have been constructed [e.g., Wüest, 1987, with a height of 31 mm].

4.1.6 Power requirements

Controllers for hot ion gauges are designed such that if the measured pressure exceeds the allowable upper limit, the sensor head is turned off in order to prevent burning the filament or damaging the sensor head. A possible set-up of controller components is shown in Figure 4.3. Typical operating conditions are shown in Table 4.1 (next page).

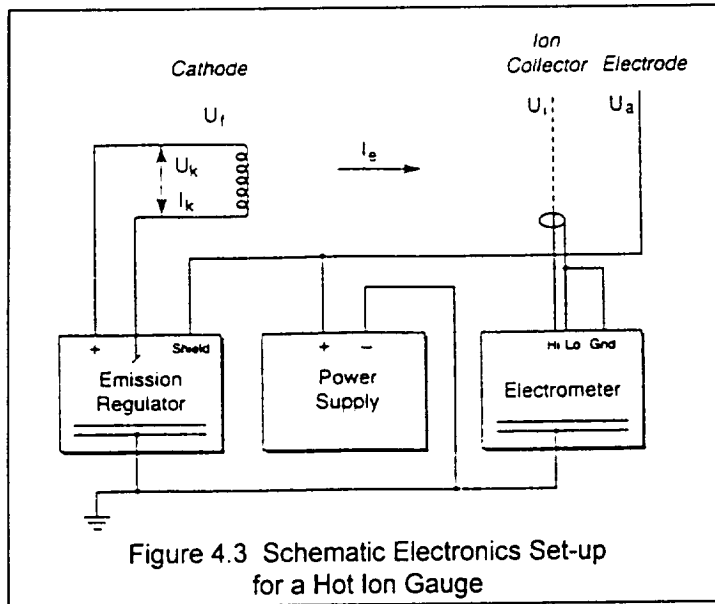


Figure 4.3 Schematic Electronics Set-up for a Hot Ion Gauge

Ion gauges usually have a degas feature, which cleans the surfaces from absorbed matter through intense electron bombardment. This feature drives the power requirements of the controller box. Degassing is important in the case when precision and absolute pressure readings are required.

4.2 Cold Cathode

4.2.1 Principle of operation

Some cold cathode ionization vacuum gauges function according to the principle of the inverted magnetron [Haefer, 1955]. An independent gas discharge is maintained in the measurement chamber through the application of a high voltage. A magnetic field penetrating the measurement chamber at the same time forces the electrons along a spiral path from the cathode to the anode. This lengthening of the path followed by the electrons assures a sufficient amount of ionizing collisions between the electrons and the gas molecules to maintain a gas discharge even at low density gas atmospheres. When the type of gas in the atmosphere is known, and the anode voltage and the magnetic field are constant, the discharge current is a measure of the prevailing pressure. A schematic of such a cold cathode ion gauge is shown in Figure 4.4.

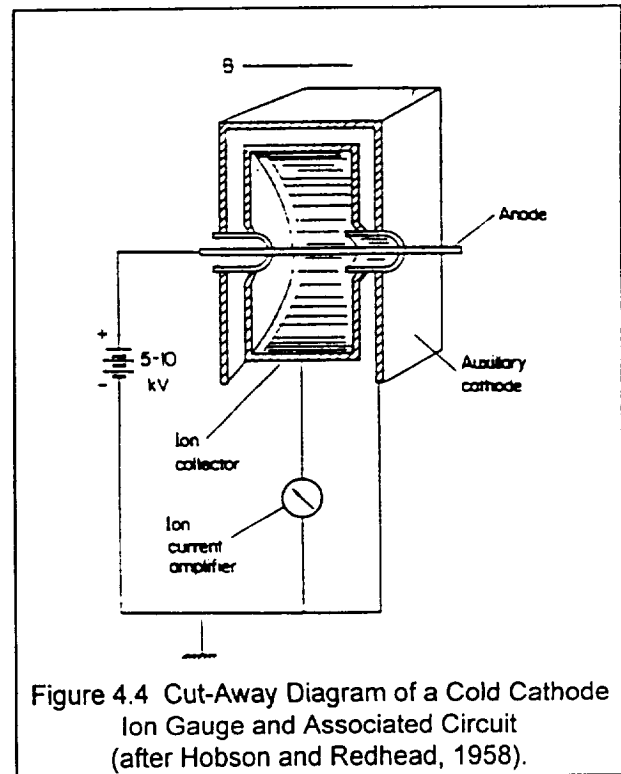


Figure 4.4 Cut-Away Diagram of a Cold Cathode Ion Gauge and Associated Circuit (after Hobson and Redhead, 1958).

Table 4.1 Typical Values of Hot Ionization Gauges

	Conventional Triode	Bayard-Alpert	Cold Cathode
Pressure Range ^{1,2} (mbar)	$10^6 - 1$	$10^{12} - 10^2$	$5 \times 10^{11} - 5 \times 10^5$
Response time (sec)			1-2
Reproducibility			± 1.5 to $\pm 5\%$
Operational data			
Heating voltage (depending on filament used) (V)	2-3	4-6	
Heating current (A)	2-3	2-4	
Filament Potential (V)	+35-50	30-50	
Grid voltage (V)	+160	+150-180	
Grid current (emission) (mA)	0.005-10	0.004-10	
Collector potential (V)	0	0	
Modulator potential (V)	$\frac{3}{4}$	0-150	
Electron bombardment			
Approx. grid voltage (to GND) (V)	+500	+600	
Max. collector voltage (to GND) (V)	500	600	
Degassing current (mA)	20-25	25-100	
Bakeout temp. max.	90-450	120-450	150-250
Gauge head without cable (°C)			
Materials			
Flange	A1, Stainless Steel	Stainless Steel	Stainless Steel
Feedthrough	Araldit, A1 ₂ O ₃	A1 ₂ O ₃	A1 ₂ O ₃
Seal	Viton, Cu	Cu	Viton/Cu
Cathode	Thoriated, Iridium	Thoriated Iridium/Tungsten	$\frac{3}{4}$
Ion collector	Tungsten	Tungsten	
Electron collector	Molybdenum	Platinum-Iridium	
Filament holder	Nickel	Nickel/Molybdenum	$\frac{3}{4}$
Radiation load head without cable (rad)	$10^8 - 10^9$	$10^8 - 10^9$	
Nude head			
Length above flange (mm)	50-83	59-83	71-98
Diameter of (nude) head (mm)	25-29	27-32	65
Weight (head) (kg)	0.3-0.5	0.1-0.5	0.5-0.8

¹ Range shown may not necessarily be covered with one sensor head.

² Typical pressure at 300 km altitude is approx. 10^{-7} mbar.

The expression for the absolute sensitivity is

$$I^+ = S \cdot P^n \quad (3)$$

where I^+ is the positive ion current collected at the cathode, P is gas pressure, and n is a numerical exponent.

4.2.2 Advantages and limitations

Cold cathode high vacuum gauges are particularly reliable and robust because they have no filament to burn out. Cold cathode high vacuum gauges cannot identify a particular mass.

4.4 Photoionized Ion Gauge

4.4.1 Principle of operation

Instead of using a hot filament which ionizes all gases according to their ionization cross-section, a narrow line light source, such as a xenon lamp, is used in a photoionized ion gauge which ionizes only gases that have an ionization potential lower than the lamp line energy. This way an ion gauge can be made more selective to the partial pressure of a particular gas.

4.4.2 Size

Through the replacement of a filament with a lamp, the size of the sensor head increases.

4.4.3 Power

It is anticipated that for the same efficiency the power requirement will be somewhat higher for a photoionized ion gauge than for the standard ion gauge.

4.5 Semiconductor Ion Gauge

The heart of a semiconductor ion gauge is a n-type semiconductor pill. If air flows through the detector, the pill surface adsorbs oxygen. An exchange of charges takes place, increasing the ohmic resistance of the pill. Since the partial pressure of oxygen in the air remains approximately constant, a state of equilibrium is obtained. If an easily inflammable gas, such as hydrogen, CO, etc., strikes the pill surface, positive charges are generated, decreasing the resistance. These processes are reversible.

4.6 Selectivity to Ammonia

As noted above, an ionization gauge is calibrated for a particular gas and will give inaccurate pressure readings for a different gas. An ion gauge as a pressure or density measurement device does not allow the discrimination between masses or species. If the species or composition of the gas is required, a mass resolving instrument is needed, such as a mass spectrometer or a spectrograph.

4.7 Advantages and Disadvantages

Table 4.2 shows a comparison of different ion gauge types.

Table 4.2 Comparison of Ion Gauges

	Cold Cathode	Conventional Triode	Bayard-Alpert	Photoionized Ion Gauge	Semiconductor Ion Gauge
Pressure range (mbar)	$10^{-11} - 5 \cdot 10^{-3}$	$10^{-6} - 1$	$10^{-12} - 10^{-2}$	Not yet known	$10^3 - 10^6$
Only specific to NH_3	No	No	No	To a small degree, interference is a problem still.	To a small degree.
Advantages	<ul style="list-style-type: none"> • simple rugged construction • higher sensitivity • no filament to burn 	<ul style="list-style-type: none"> Higher pressure limits 	<ul style="list-style-type: none"> Lower pressure limits 	<ul style="list-style-type: none"> Some interference is eliminated by controlling the ionization energy of the light source. 	<ul style="list-style-type: none"> Rugged construction
Disadvantages	<ul style="list-style-type: none"> Non-linearity of collected current as function of pressure. High voltages involved (3 keV). Higher power consumption heavier (magnet). 	<ul style="list-style-type: none"> Linear ion current with lighter weight Probably lowest power requirement 	<ul style="list-style-type: none"> Filament can burn out 	<ul style="list-style-type: none"> No commercial sensor heads available. Heavier (lamp) 	

5.0 Evaluation of Baseline and Alternative Ammonia Leak Detection Methods

5.1 Instruments Evaluated

The instruments evaluated in this study are listed in Table 5.1. The list was derived from (i) the previous study [Jolly and Deffenbaugh, 1989], (ii) suggestions by NASA-JSC personnel, and (iii) a literature review. All the instruments can operate in a hard vacuum and be integrated into a hand-held device.

Table 5.1 Instruments Evaluated in Trade Study

Instrument	Principle of Operation
Ion gauge (baseline instrument)	measures density (or pressure) of gas
"Selective" ion gauge	measures density of gas selectively ionized by cut-off level of optical excitation
Mass spectrometer	selects gas on the basis of atomic mass and measures density of that gas with an ion gauge
Infrared absorption gauge	laser light tuned for absorption by ammonia; receiver examines transmitted light for ammonia absorption bands
Infrared fluorescence gauge	laser light tuned to excite ammonia into fluorescence; optical receiver detects fluorescence
Disclosing paint	paint changes color in the presence of ammonia

5.2 Trade Study of Ammonia Leak Instruments

NASA-JSC suggested twelve criteria to be used in judging the potential leak-locating instruments. The relative importance of each of the criteria varied from one to three, depending upon how important each criterion was relative to the others. Furthermore, if any instrument received a score of zero for any of the criteria, it was deemed to have failed and was not a viable instrument. The bases for the scores are reviewed below. The review panel was composed of SwRI personnel who had demonstrated expertise in designing, fabricating, and using one or more of the instruments.

The scores for this trade study are shown in Table 5.2 (next page). As can be seen from the table, the mass spectrometer instrument received the highest total, primarily because of its sensitivity to ammonia. The disclosing paint and the selective ion gauge received the second and third highest totals. The baseline ammonia gauge, which received a score of zero for lack of sensitivity to ammonia, failed.

5.3 Discussion of Trade Study Scores

The criteria for each instrument are discussed separately, to the extent possible, in the following sections. In some cases, as needed for clarity, the criteria are preceded by a discussion of the instrument.

5.3.1 Ion gauge

The measurement principle of a hot cathode ionization gauge relies on gas ionization. Emitted electrons from the hot cathode collide with gas molecules in the active region of the gauge, ionize some of them and produce a measured ion current. An ion gauge is a pressure measuring device only. A complete description is presented in Section 3.0 of this report.

Selectivity. Ion gauges are in principle density measurement devices. The density can be interpreted as total pressure by an appropriate conversion factor. A conventional ion gauge *cannot discriminate* between the atomic masses (or species) of the various gas molecules that generate the total

Power use. A simple, hand-held ion gauge is expected to require no more than about two watts. An above-average score of 4 was awarded.

Response time. The response time depends on the opening area of the gas inlet (to accumulate a sufficiently large sample) and the electronic processing of the signal. The total time can vary from nearly instantaneous to several seconds. This time is close to the shortest of all the instruments, so a score of 4 was awarded.

Vacuum compatibility. An ion gauge head is fully compatible with space vacuum. Electronics have been flown in space before as well. Therefore, a maximum score of 5 was awarded.

Temperature compatibility. Operational requirements for the electronics require the electronics and battery pack to be maintained in the range of about -20°C to 50°C. This range is near the best of the investigated instruments and includes most of the anticipated space range, so a score of 4 was awarded.

Geometry. The biggest component is the space-qualified battery. Ion gauges can be purchased in packages of less than 100 x 65 x 65 mm. The electronics package is estimated to be 75 x 50 x 50 mm, based on conventional components. The total package size is estimated to be among the smaller of the instruments, and the instrument should be easily transported and manipulated by hand. A score of 4 was therefore awarded.

5.3.2 Selective ion gauge

For a selective ion gauge, an attempt is made, using a narrow band optical excitation line, to ionize only entering gas particle of the desired species. Ammonia, for example, has a first ionization potential of 10 eV. Unfortunately, other gases in the ISSA environment have first ionization potentials close to 10 eV; as one example, nitrogen tetroxide, a common attitude control engine propulsion fluid, has a first ionization potential of 9.8 eV. For this reason, the panel concluded that the selectivity of a selective ion gauge, although better than a conventional ion gauge, falls considerably short of what is needed. Furthermore, at the present, selective ion gauges are laboratory-development items, and thus are not commercially available.

Criteria. In most respects, the characteristics and therefore the score of a selective ion gauge are similar to a conventional ion gauge. For the reasons discussed above, the scores of a selective ion gauge *were reduced* slightly, compared to a conventional ion gauge, for the criteria of development cost, complexity, technology readiness, and power use. The score for the selectivity criterion *was increased* slightly, to one, compared to a conventional ion gauge.

5.3.3 Mass spectrometer

A mass spectrometer separates a gas mixture into separate streams by atomic weight. In that way, it can be made selective to ammonia (and other species that have a similar atomic weight). The spectrometer is used in conjunction with a conventional ion gauge to detect the selected species.

Selectivity. Depending on the design, a mass spectrometer can be highly selective. A miniature quadrupole design has a resolution of 1 atomic mass unit over a range of 2 to 65 amu. A Mattauch-Herzog double focusing unit can have a resolution of 0.5 amu at 50 amu. This selectivity is near the highest of all the investigated instruments, but there is still a small probability of sensing gases other than ammonia; thus, a score of 4 was awarded.

Sensitivity. A density sensitivity equivalent to 10^2 molecules/cm³ can be obtained. This is the highest sensitivity of all the instruments; thus a score of 5 was awarded.

Development cost. A mass spectrometer is a more complicated instrument than the baseline ion gauge; its development costs are correspondingly higher. A typical neutral mass spectrometer contains an ionization source, a mass selector, and an ion detector. A middle-range score of 3 was awarded.

Sensing geometry. Compared to an ion gauge, the angular acceptance of a mass spectrometer is slightly reduced because of the finite gap width of the mass selector. However, the difference is small enough that the same score of 4 as for the ion gauge is justified.

Accuracy. The accuracy of mass spectrometer is better than 10%. This is the best of the investigated instruments, so a score of 5 was awarded.

Complexity. Compared to the baseline ion gauge, a mass spectrometer is a more complex instrument because of its electron bombardment source and the need to provide both an electric and a magnetic field as well as a high-voltage detector. The complexity is, however, less than that of several of the competing instruments, so a middle-range score of 3 was awarded.

Technology readiness. Mass spectrometers have flown on many space missions. For a hand-held instrument, however, a limited amount of development will be needed to reduce the size of some components. There are commercially available, hand-held spectrometers on the market. An above-average score of 4 is justified.

Power use. For a Mattauch-Herzog mass spectrometer, the required power is estimated to be six to eight watts (based on an instrument design proposed for the Mars lander). The power use of a miniature quadrupole design is slightly higher and estimated to be seven to nine watts. A middle-range score of 3 was awarded.

Response time. The response of a mass spectrometer is nearly instantaneous. The highest score of 5 is justified.

Vacuum compatibility. Most of the complexity of commercial units is providing this vacuum. The spectrometer is compatible with a hard vacuum. The sensor head, in fact, must be used in a vacuum. A score of 5 was awarded.

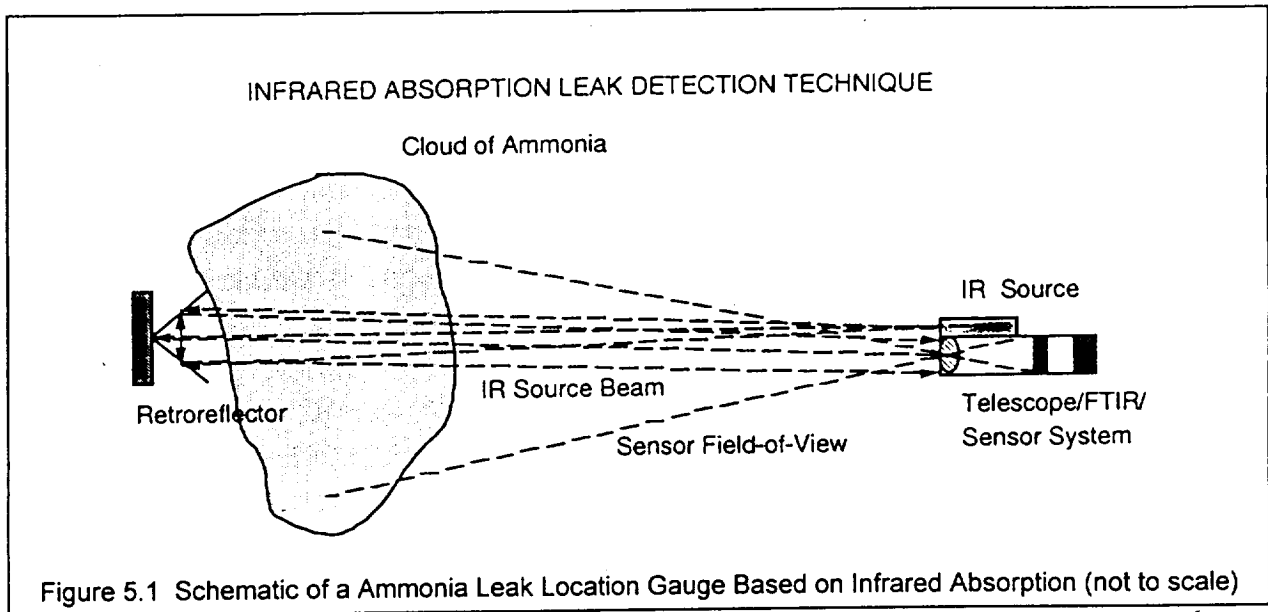
Temperature compatibility. The compatibility of the electronics is similar to that discussed for an ion gauge. Thus, a score of 4 was awarded.

Geometry. A neutral gas mass spectrometer can be packaged in a volume of 180 x 180 x 50 mm, and the electronics can be packaged in a volume of 190 x 190 x 75 mm. The battery is not included in these estimates. The overall size is still easily hand-held, but, because of the larger size compared to the baseline ion gauge, a score of 3 was awarded.

5.3.4 Infrared absorption gauge

The fundamental physical principle of the operation of an infrared absorption gauge is compatible with ammonia leak location. A schematic of such a gauge is shown in Figure 5.1. Ammonia has a number of strong absorption bands (due to vibrational states of the ammonia ground-state molecule) in the infrared wavelength region near 3 μm and near 6 μm and between 8 to 14 μm . The IR source (e.g., a laser) is used to send a beam through the gaseous environment, which excites any ammonia molecules in the gas. With the receiver at the same location as the source (as shown in Figure 5.1), various corner reflectors would be required in an array around the volume that is being investigated to reflect the light back to the receiver after passing through the gas cloud. The receiver essentially detects whether any of the light from the source has been absorbed by ammonia molecules. It would have to incorporate an IR-sensitive photodetector and a Fourier Transfer Infrared Spectrometer (FTIR). To be useful, the column length of the ammonia cloud and the integration time of the instrument must be sufficiently large to generate a detectable signal.

Selectivity. The capability of the gauge to select and detect ammonia, while excluding other gases, is about the same as a mass spectrometer. Thus, a score of 4 was awarded.



Sensitivity. The use of this gauge in an environment having a pressure of the order of 10^{-6} torr depends on the absorption cross-section of an ammonia molecule, the number density of the ammonia cloud, and the total length of the light path through the cloud, as well as on the sensitivity of the receiver. The volume and the low number density of typical ammonia clouds that might occur for ISSA make the sensitivity of the gauge marginal. Thus, a low score of 1 was awarded.

Development cost. A flight-qualified, hand-held, laser/telescope/detection system combined with a FTIR is at present merely a concept. Hence, a low rating of 1 was awarded for this criterion.

Sensing geometry. Sensing can only be accomplished over paths between fixed retroreflectors distributed over ISSA and the transmitter/receiver instrument. Many, perhaps hundreds of retroreflectors, will be required. Hence, a low score of 1 was awarded.

Accuracy. The accuracy of the gauge depends on the signal-to-noise ratio of the detected absorptions. Because of the low signal-to-noise ratio, very long integration times will be required to achieve a minimum level of accuracy. For that reason, and compared to the sensitivity of the other instruments, a moderately low score of 2 was awarded.

Complexity. The gauge, which requires some kind of laser or IR-emitting device, a receiver and telescope, a receiver, and a FTIR is the most complex of all the instruments surveyed. A score of 1 is therefore justified.

Technology readiness. Many of the instrument components are available (although perhaps not in flight-qualified form), but an integrated package for space applications is not. A moderately low score of 2 was awarded.

Power use. Power is required to operate the focal plane and its associated electronics, the laser or IR source, and the electronics (which are considerably more sophisticated than for the baseline ion gauge). Quantitative power estimates were not made, but the total will be significantly greater than for the baseline gauge. Hence, a score of 2 was awarded.

Response time. As discussed previously, the response time of this gauge is inherently associated with the low signal-to-noise ratio. It is estimated, for typical ammonia leak cloud densities, that the response time will be of the order of minutes or even hours.

Vacuum compatibility. With some development and packaging, the gauge can be made compatible with the vacuum of space. A middle-range score of 3 was awarded.

Temperature compatibility. The more sophisticated electronics of the gauge, compared to the baseline ion gauge, makes the gauge somewhat more sensitive to temperature extremes. A score of 3 is justified.

Geometry. The overall size of the gauge is estimated to be the largest of all the instruments investigated, and may perhaps exceed the "hand held" criterion. A moderately low score of 2 is justified.

5.3.5 Infrared fluorescence gauge

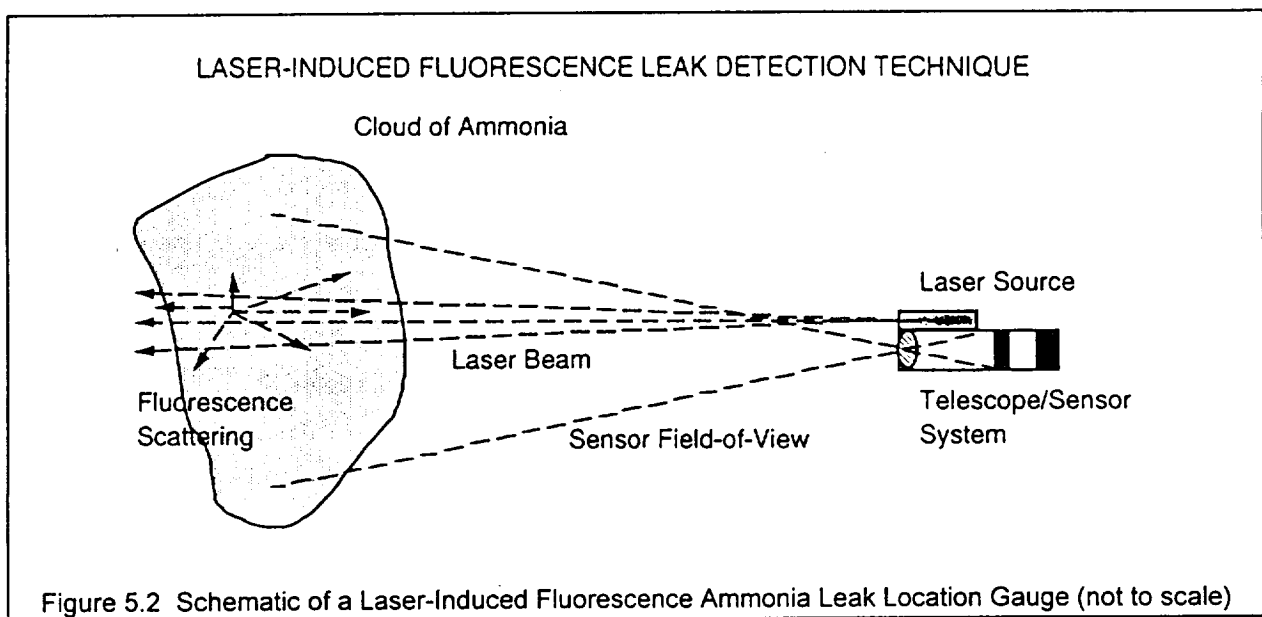
The fundamental physical principle of the operation of an infrared fluorescence gauge is also compatible with ammonia leak location. A schematic of such a gauge is shown in Figure 5.2. As stated earlier, ammonia has a number of strong absorption bands (due to vibrational states of the ammonia ground-state molecule) in the infrared wavelength region near $3\ \mu\text{m}$ and near $6\ \mu\text{m}$ and between 8 to $14\ \mu\text{m}$. A laser tuned to one of these wavelengths would stimulate ammonia molecules to a higher vibrational state; when the molecules relax back to the ground state, photons having a longer infrared wavelength region would be emitted (i.e., the molecules would fluoresce). For example, if an ammonia molecule is excited by $2.9\ \mu\text{m}$ photons, the de-excitation would occur at $6.1\ \mu\text{m}$. An optical receiver capable of detecting the resulting fluorescence could be used to locate ammonia leaks. A single, hand-held instrument could raster the laser beam to sweep out a three dimensional volume around the instrument. The complete instrument would require a telescope and an infrared-sensitive detector (having a narrow band filter at the expected fluorescence wavelength). As an additional benefit, the ammonia cloud could also be imaged as well as detected and located.

The infrared fluorescence gauge shares many of the attributes of the infrared absorption gauge. However, it is judged to be somewhat more selective in excluding other species, somewhat less complex, and, because of its three-dimensional sensing capability, to have the highest of all sensing geometry features. It is also more probable that a hand held gauge could be developed. The scores, thus, are somewhat higher for all these criteria than for the infrared absorption instrument.

5.3.6 Disclosing paint gauge

A unique ammonia sensitive paint has been developed for NASA-JSC [Graef, Mallow, Caceres, 1993]. This "litmus paper type" coating changes color when exposed to trace amounts of ammonia.

Selectivity. Test results for the paint show that it will change colors only to ammonia and is unaffected by the presence of other contaminant gases, thus a score of 5 was awarded.



Sensitivity. While there is a range of concentration that results in a degree of color change, this range is relatively small. A color change was observed at concentrations as low as 1 part per million. This is not as good as the mass spectrometer and only slightly lower than the ion gauge, so it received a score of 2.

Development cost. Integration cost of this paint into a hand-held device is relatively straightforward. The only development cost is the final formulation of the paint composition to balance all of competing design requirements. It, therefore, received a score of 4.

Sensing geometry. A simple hand-held enclosure is required to "capture" sufficient number of ammonia molecules. This geometry is small and relatively simple, thus, a score of 4 was awarded.

Accuracy. This is basically a go or no-go type of indication. It, therefore, cannot quantify concentration. A score of 1 was, therefore, awarded.

Complexity. The disclosing paint does not require any electronics and is, therefore, the least complex of any of the gauges evaluated. It was awarded a score of 5.

Technology readiness. No prior flight experience exists, but a breadboard demonstration has been produced and tested. Its technology readiness is not as good as the baseline ion gauge, but better than the two infrared devices. A score of 3 was awarded.

Power use. No power is required, thus, a score of 5 was awarded.

Response time. The response time is good; however, not as good as the mass spectrometer. It was awarded a score of 4.

Vacuum compatibility. This is the one major concern for the disclosing paint. The initial formulation of the paint was exposed to various levels of vacuum. At 10^{-6} torr and 150°F, the paint lost an order of magnitude sensitivity over the course of a 6-week period. Since the original purpose of the paint was a twenty year indication for the external utility trays of Space Station Freedom, it was deemed to have an unacceptable life. However, for a hand-held device that is to be used for a one-day-at-a-time EVA, this is not as detrimental. A series of coupons could be used, thus, it was awarded a score of 1.

Temperature compatibility. Since this is a chemical sensitivity, its temperature compatibility may be limited. A thermal cycle test was performed with no sensitivity loss over a two-week period. A score of 2 was awarded due to the limited data available.

Geometry. There are no real geometry limits. This "device" could be as simple as attaching small circular samples to the crew member suite or integration into a small covered sniffer the size of the crew member's hand. It was awarded a score of 5.

6.0 Conclusions and Recommendations

The basis of this study is that the ammonia inventory management system senses loss of ammonia. A crew member will, then, perform an EVA with a hand-held sniffer to locate the ammonia leak external to the station. In the absence of any station vents, a pressure measurement device would be sufficient to locate this leak if the crew member was within several feet of the leak. An ion gauge is an ideal and simple device for this type of pressure detector. It was selected by the prime contractors as the baseline approach. However, based on the venting and offgassing data provided by NASA-JSC, the pressure environment external to the station is such that a pressure or density device would have to be within inches of the leak to detect it, and also sufficiently far enough away from the plumes of vents and offgassing sources. This does not appear to be feasible, so an ion gauge is not, therefore, a practical solution.

The other types of techniques were traded off against the ion gauge to identify better alternatives. From a pure technology point of view, a hand-held mass spectrometer was found to be clearly superior to all other approaches, primarily because it can accurately sense the composition of the different gases and

will require relatively little development. The detection of composition not pressure would be more successful in the predicted environment external to the station. Prior attempts at developing a mass spectrometer for this type of application have been problematic. Mass spectrometers have, however, been developed as science instruments for a number of applications. The limited task of locating an ammonia leak should not be difficult for a device similar to commercial units now on the market.

Two other approaches ranked below the mass spectrometer do appear feasible. One is a unique disclosing paint that functions like a "litmus paper" for trace amounts of ammonia, and the other is a selective ion gauge that only ionizes gases with ionization potential below a selective threshold. Neither of these devices has a commercial version, and therefore, are more risky.

The recommended leak detector for this application is the hand-held mass spectrometer.

References

- Fuchs, H., and Legge, H. (1979), *Acta Astronautica*, **6**, 1213-1226.
- Graef, R., Mallow, W. and Caceres, W. (1993), SwRI Final Report, Project 04-2529.
- Haefer, R. (1955), *Acta Phys. Austriaca*, **9**, 200.
- Hobson, _, and Redhead, P. (1958), *Can. J. Physics*, **36**, 21.
- Jolly, D., and Deffenbaugh, D. (1989), SwRI Final Report, Project 04-2525.
- Knight, C. J. (1976), *J. Fluid Mechanics*, **75**, 3, 469-486.
- Mann, B. L., and Stoll, O. T. (1964), SAE Paper 912D.
- McCulloh, K., and Tilford, C. (1981), *J. Vac. Sci. Technol.*, **18**, 3, 994-996.
- Mikatarian, R. R., and Anderson, R. G. (1965), *Proc. AIAA Unmanned Spacecraft Conference*, **12**, 225-229.
- Poulter, K., and Sutton, C. (1981), *Vacuum*, **31**, 3, 147-150.
- Redhead, P. (1969), *J. Vac. Sci. Technol.*, **6**, 5, 858-854.
- Steddum, F., Maples, D., and Donovan, M. (1970), *NBS Space Simulation*, **56**, 905-914.
- Tilford, C. (1983), *J. Vac. Sci. Technol.*, **A1**, 2, 152-162.
- Tilford, C. (1985), *J. Vac. Sci. Technol.*, **A3**, 3, 546-550.
- Weinman, J. (1966), *Rev. Sci. Instrum.*, **37**, 636.
- Wüest, M. (1987), Dissertation, Universität Bern, Switzerland.